ADV Preview Based Nonlinear Predictive Control for Maximizing Power Generation of a Tidal Turbine with Hydrostatic Transmission

Xiuxing Yin and Xiaowei Zhao

***Abstract*—As the development of tidal turbines attracts more and more attention in recent years, reliable design and efficient control of tidal turbines are becoming increasingly important. However, the majority of existing tidal turbines still utilize traditional fixed ratio geared transmissions and the associated control designs focus on simple feedback controllers that use measurements or possibly estimates of the turbine itself or current local tidal profile. Therefore, the measurement and control are inevitably affected by the inherent delay with respect to the current tidal speeds. This paper proposes a novel tidal turbine with continuously variable speed hydrostatic transmissions and a nonlinear predictive controller that uses short-term predictions of the approaching tidal speed field to enhance the maximum tidal power generations when the tidal speed is below the rated value. The controller is designed based on an offline finite-horizon continuous time minimization of a cost function, and an integral action is incorporated into the control loop to increase the robustness against parameter variations and uncertainties. A smooth second order sliding mode observer is also designed for parameter estimations in the control loop. A 150 kW tidal turbine with hydrostatic transmission is designed and implemented. The results demonstrate that the averaged generator power increases by 6.76% with this preview based nonlinear predictive controller compared with a classical non-predictive controller.**

***Index Terms*—Tidal turbine; Hydrostatic transmission; Sliding mode observer; Nonlinear predictive control, Acoustic doppler velocimetry preview**

I. Introduction

THE exploitation of tidal energy offers great opportunities in meeting the world's long term renewable power and greenhouse gas emission reduction targets. Currently, the most promising tidal energy technology is to directly generate electricity from tidal currents by using a tidal turbine. In recent years, tidal turbine technology has experienced a rapid expansion. Among various types of tidal turbines, horizontal axis tidal turbine tends to have the highest efficiency ranging from 39% to 48% in comparison with its vertical axis countertype [1]. The existing research on horizontal axis tidal turbines prevails and examples of recently developed tidal turbines include the 1.2 MW SeaGen developed by the Marine Current Turbines, the 1 MW TidEl from the SMD Hydrovision, the 250 kW Open Hydro open center turbine, and the 1.2 MW Delta Stream from the Tidal Energy Ltd [2]. The SeaGen 1.2 MW turbine has been installed at Strangford Lough, UK, and can generate approximately 6 GW of electricity per year [3]. The TidEL turbine floats and is restrained by mooring chains to the sea bed, which differs from most tidal turbines that are fixed to piles driven into the sea bed. The TidEL incorporates two buoyant 500kW generators that are joined together by a cross beam to give a total power capacity of 1 MW at 2.3 m/s flow rates with a 0.7 m/s cut-in tidal speed [4]. The 250 kW Open Hydro open center turbine has been installed in a test rig with two steel monopoles grouted into sockets drilled into the seabed. The turbine is six meters in diameter and can be grid connected to generate electricity to the national grid in the UK [5]. The Delta Stream unit consists of up to three tidal turbines mounted on a triangular steel main base. The total capacity of a unit can amount to 1.2 MW when three independent horizontal tidal turbines are installed on each nacelle [6]. Other tidal turbines have been investigated and tested in the European Marine Energy Centre in the UK [7]. The results indicate that horizontal axial turbine systems seem better suited for extracting tidal energy, and the ducted turbine with diffuser and ventury system can generate more power than the open type, but it has higher first investment cost.

However, most of the existing tidal turbines are commonly equipped with gearbox drive trains and the turbine transmission ratio cannot be continuously varied in accordance with incident tidal stream speeds. Therefore, hydrostatic transmission with continuously variable ratios seems to be a promising alternative to fixed ratio gearbox transmission for tidal turbines. The hydrostatic transmission based tidal turbine (HTT) is an attractive option in terms of relatively high reliability and high controllability. However, the HTT is very rarely reported in the existing literature. In [8], the performance of a digital displacement technology based HTT was investigated. However, the work only focuses on the hydraulic transmission while other aspects of tidal energy generation are not presented to the same level of detail. In [9], the hydrodynamics of a HTT was analyzed at first and its power output characteristics were predicted. The simulation and test results of a 20 kW HTT have shown that the hydrostatic transmission efficiency exceeds 70%. However, the work only aims at the stabilization of the tidal power output while the power maximization strategy was not investigated. The used HTT was designed by using a fixed displacement hydraulic pump in a simple hydraulic system,

Xiuxing Yin and Xiaowei Zhao (corresponding author) are with the School of Engineering, the University of Warwick, Coventry, CV4 7AL, U. K. Emails: x.yin.2@warwick.ac.uk, xiaowei.zhao@warwick.ac.uk. This work was funded by the UK Engineering and Physical Sciences Research Council (grant numbers: EP/R007470/1 and EP/S000747/1).

which may not function well under harsh tidal stream conditions. In addition, the whole dynamics model of the HTT was not detailed. In [10], a time domain simulation of a low speed vertical axis HTT was presented by using MATLAB/Simulink. The simulation is useful, but the detailed dynamics modelling and control were not presented.

The efficiency of a tidal turbine is crucial in determining its economic potential and length of payback. The tidal turbine efficiency is not only affected by blade or hydrofoil designs, but also is highly dependent upon specific control strategies. Existing literature in the turbine control field focuses on control strategies using measurements from the turbine itself. In [11], control performance of pitch and stall regulated tidal stream turbines was investigated. The results indicate that the pitch regulated turbine would be a more attractive solution for tidal energy development. However, the used assumption that the two types of tidal turbines are comparable requires further investigation. In [12], feedback flux-weakening control and torque control for a fixed-pitch marine current turbine above the rated tidal speed were investigated and compared. The simulation results show that torque control scheme works more efficiently than speed control scheme and is more capable of limiting the generator produce power to the rated value at steady-state. However, the control methods were not investigated at low tidal speeds. In [13], a passive pitch controller was designed to improve structural performance and increase lifetime of the tidal turbine. The results indicate that passive pitch control of tidal turbine blades has the potential to improve overall system performance. However, no fluid cavitation in the blades was considered in the study. In [14], a robust nonlinear second-order sliding mode control was proposed for a turbine simulator. The obtained results are encouraging in the validation of the simulator. However, vertical-axis turbine models were not included in the validations. In [15], a regulation method of tidal power was presented and validated based on results from simulations using GH Tidal Bladed. The simulation results showed that near-constant power output with variations of less than 0.6% could be achieved by using the method. However, the method is not applicable to generic types of turbine blades. In [16], a control strategy was proposed to efficiently extract energy from a fixed-pitch tidal turbine associated with a 5-phase permanent magnet generator (PMG) in both healthy and faulty modes. The results show that the 5-phase PMG can operate in faulty mode while maintaining relatively good performance over a high range of speed. However, the influence of harmonics on the performance of the control strategy was not investigated.

In practice, tidal turbine systems are inherently nonlinear and the above existing control methods may not be adequate for highly nonlinear turbines within large operating regimes. Also, there is an inherent delay between the measured tidal stream speeds and the applied control actions. These drawbacks coupled with increasingly stringent demands on tidal power quality have highly spurred the development of nonlinear predictive control (NPC) that is an optimization-based control using predictions of future system outputs. The NPC has been applied in the field of preview wind turbine control based on the LIght Detection And Ranging (LIDAR) remote sensing technology which enables measurements of upstream wind speeds. In [17], a NPC was designed by using LIDAR preview which has shown great advantage compared with a baseline controller. However, the performance of the controller in comparison with a LIDAR-assisted feedforward controller is not clear. There are also some other preview based control methods applied in wind turbine research. In [18], an adaptive feedforward controller and a non-adaptive feedforward controller were designed to augment a collective pitch proportional-integral (PI) feedback controller for wind turbine rotor speed regulation. The results have shown that the feedforward control gives better performance than the baseline PI feedback control in both tower and blade bending moment mitigation. However, the feedforward control was not investigated for region 2 operation where the wind turbine is operating below the rated wind speed. In [19], preview-based disturbance feedforward control was investigated for wind turbine load mitigation. The obtained results showed that excellent performance gains using the control are possible with reasonable pitch rates. However, the results using more realistic wind measurements showed that the control performance degrades without better processing of measurements and further controller optimization. In [20], the potential of using previewed wind speed measurements for damping wind turbine fore-aft tower oscillations was investigated. The results showed that a 31% improvement in terms of the damage equivalent load can be achieved by using the availability of 1.3 s preview. However, the previewed measurements were not useful when their bandwidths do not exceed the natural frequency of the tower. In [21], a non-linear pitch control strategy including tower load reduction and LIDAR preview measurements was proposed for wind turbines when the wind is above rated. The simulation results showed that the non-linear controller outperforms the baseline gain scheduled PI controller. However, the performances of the non-linear controller were not compared with other LIDAR preview control methods.

The aforementioned LIDAR preview based NPC designs in [17] were used for wind turbine with gearbox drivetrain which cannot be directly used for tidal turbines with hydrostatic transmission. In addition, although much effort has been made in NPC by using more accurate prediction and optimization models, the NPC optimization problem must be solved online, resulting in high computational complexity and control delays at each sampling period. The optimization problem is generally nonconvex due to nonlinear model, which may mean an online solver is unable to find a near-optimal feasible solution in time. Therefore, the conventional NPC designs need to solve nonlinear and non-convex optimization problems online, and the computational burden for solving these problems depends on system order, non-linearity, the horizon length and the used nonlinear optimization solver, and is thus quite large and is not suitable for real time practical implementations.

Furthermore, despite the excellent predictability of the mean tidal speeds and directions, the turbulent tidal gusts are chaotic and cannot be predicted well for more than a short distance into the future. This poor predictability of turbulent flows within a tidal stream essentially motivates advanced online predictive control of a tidal turbine.

Therefore, this paper aims at the design, detailed modelling and nonlinear predictive control of a new horizontal axis HTT with continuously variable speed hydrostatic transmission. The turbine dynamics are modelled in details by combining governing equations of the turbine rotor and the hydrostatic transmission. An optimal NPC is then designed to achieve the maximum tidal power generation by minimizing a predictive cost function along a finite horizon, which can also make use of predictions of future upstream tidal speed conditions through direct measurements. The designed NPC is derived by expanding the turbine model and the optimal signals in Taylor series and the control signals are explicitly given in a closed form without online optimization to expedite the computational speed for the HTT. In addition, in order to increase the robustness of the proposed NPC with respect to model uncertainties and parameters variations, an integral action is introduced into the control loop and a smooth second order sliding mode observer is designed and implemented online for HTT parameter estimations, which guarantees the overall control performance. Comparison tests based on a 150 kW HTT for the cases with and without preview predictive control are performed.

To the best knowledge of the authors, there are no investigations on NPC design for tidal turbines, not to say for HTTs. The main contributions of this paper consist of the following elements.

(a) A horizontal axis HTT is proposed, designed, modelled and finally validated to enhance the tidal turbine performance. In contract to the existing HTTs [8]-[10], the displacements of the hydraulic pump and motor can both be regulated simultaneously and continuously in the proposed HTT, which allows variable speed control of the tidal turbine rotor while maintaining constant generator rotation speed. Unlike the above-mentioned works on HTT modelling, the detailed dynamics model of the HTT is investigated and presented. Therefore, the proposed HTT is more controllable and reliable, and is able to transform low variable speed tidal inputs into constant high-speed generator outputs.

(b) A NPC is proposed and derived based on the continuous minimization of a predictive cost function along a finite horizon. The optimization is performed offline and suitable Taylor series expansions are adopted for the prediction process. In contrast to conventional nonlinear model predicative control methods that need online optimizations, the implementation of the proposed NPC does not need online optimization, which significantly improve the control efficiency.

(c) An integral action is incorporated into the proposed NPC and a smooth second order sliding mode observer is designed and implemented to increase the robustness of the closed-loop system with respect to uncertainties and parameters variations.

(d) Different from conventional NPC algorithms whose robustness and stability cannot be rigorously analyzed or proved, the proposed NPC is given in a closed form, and its stability and robustness are rigorously proved and guaranteed. The proposed NPC also holds significant advantages of higher robustness, better tracking performance and lower computation burden. The proposed NPC framework is more generic and can be applied to general nonlinear systems with fast dynamics, and hence is suitable for industry implementation and can be extended to the control of various nonlinear systems with uncertainties and external disturbances.

II. THE NPC REGULATED HTT

The designed HTT is a horizontal axis tidal turbine with the turbine rotor shaft parallel to incoming tidal streams. As illustrated in Fig. 1, a high pressure closed-loop hydrostatic transmission is used in the HTT (instead of rigid gear ratio mechanical gearbox) for continuously variable speed transmissions. The hydrostatic transmission is mainly composed of a variable displacement hydraulic pump, a variable displacement hydraulic motor, a high pressure accumulator, a generator. The hydraulic pump and motor are equipped with volumetric displacement control mechanisms that can be operated to continuously change the pump/motor displacement ratio, thereby varying the hydrostatic transmission ratio. The hydraulic motor is rigidly connected to a generator for converting the pressurized hydraulic fluid power from the hydraulic pump into electricity, which eventually transforms the input kinetic tidal energy into useful electrical power output. The high pressure accumulator can be used as an energy buffer for smoothing any tidal speed or torque spikes, enabling the decoupled dynamics control of the hydraulic pump and motor.

In contrast to the existing HTTs [8]~[10], the displacements of the hydraulic pump and motor can both be regulated simultaneously and continuously in the proposed HTT. By regulating the hydraulic pump displacement in time and using the high pressure accumulator as energy buffer, the HTT can well accommodate bidirectional tidal flows and considerable short-term tidal speed variations or turbulences. This high controllability renders the HTT much more reliable under harsh tidal stream conditions in comparison with the fixed speed gearbox based tidal turbine. On the other hand, the generator speed can be maintained relatively constant by varying the hydraulic motor displacement regardless of the variable tidal flows. In this case, HTT does not need the traditional expensive power converters at the generator side. Thus its total cost may be lower than the tidal turbine with fixed speed gearbox and variable speed drives.

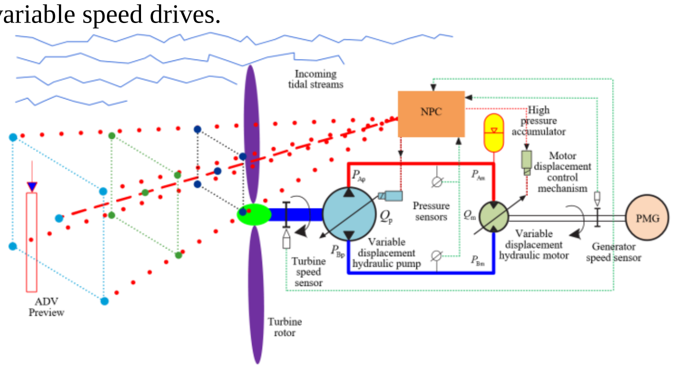

Fig. 1 Schematic of the NPC regulated HTT

Because of the high tidal turbine rotor inertia, there will be significant phase delays in the HTT control and responses with respect to incoming tidal streams. Hence, the NPC that fully utilizes the advance knowledge of the incoming tidal field will be beneficial in addressing these issues. As shown in Fig. 1, the NPC is designed to regulate the hydraulic pump and motor displacements based on the Acoustic Doppler Velocimetry (ADV) that can acquire the approaching tidal field and speed measurements in advance. The ADV with great operational flexibility and lower cost is usually located in the upstream of the turbine rotor to exploit the full available future tidal field measurements [22]. By incorporating and fully utilizing the preview tidal speed measurements, the ADV preview based NPC is able to circumvent the phase delays and therefore react earlier to incoming tidal events, potentially leading to increased power capture and lower structural fatigue loads when the tidal speed is below rated. Additional benefits of using the ADV preview based NPC are the dynamical anticipation upon future extreme events and less aggressive control actions, which lead to the reductions of mechanical loads and the overall cost of energy. By implementing the NPC, it is possible to enhance the overall turbine performance, reduce downtime and maintenance cost, and prolong the life cycle of the tidal turbine.

III. HTT Dynamics

The HTT dynamics can be obtained by combining governing equations of the turbine rotor and the hydrostatic transmission.

A. Hydrodynamics of the Turbine Rotor

The tidal power captured by the turbine rotor is given by

$$P_{\mathrm{t}} = T_{\mathrm{t}} \cdot \omega_{\mathrm{t}} = \frac{\pi \rho R^3 v(t)^2 \omega_{\mathrm{t}}}{2\lambda} C_{\mathrm{p}} \tag{1}$$

where P_{t} (W) and T_{t} (Nm) denote the turbine power and torque inputs, respectively, ρ (1025 kg/m^3) and $v(t)$ (m/s) denote seawater density and tidal flow speed, respectively, R (m) and ω_{t} (rad/s) denote the turbine blade radius and rotating speed, respectively, C_{p} and λ are respectively the power capture efficiency coefficient and tip speed ratio that is a function of tidal stream speed and turbine blade radius.

$$\lambda = \frac{\omega_{\mathrm{t}} \cdot R}{v(t)} \tag{2}$$

For a three-bladed turbine rotor, when the tidal speed is below the rated value, the efficiency coefficient C_{p} in (1) is a monotonic function of the tip speed ratio [23]. Therefore,

$$C_{\mathrm{p}} = -0.6966 \sin\left(\frac{\pi(\lambda + 0.1)}{15}\right) + 0.0037(\lambda - 3) \tag{3}$$

In the ADV preview based NPC, the inflow profile of actual tidal stream speed can be measured upstream of the tidal turbine rotor and hence the optimal turbine rotation speed is

$$\omega_{\mathrm{topt}}(t) = \frac{\lambda_{\mathrm{opt}} \cdot v(t)}{R} \tag{4}$$

The optimal turbine torque that corresponds to the optimal turbine speed is therefore

$$T_{\mathrm{topt}} = \frac{\pi \rho R^3 v(t)^2}{2\lambda_{\mathrm{opt}}} C_{\mathrm{pmax}} \tag{5}$$

where C_{pmax} is the maximum power capture efficiency coefficient of around 0.5.

B. The Hydraulic Pump

The dynamics of the two coupled components are

$$T_{\mathrm{t}} - D_{\mathrm{p}}\left(P_{\mathrm{Ap}} - P_{\mathrm{Bp}}\right) - c_{\mathrm{fp}}\omega_{\mathrm{t}} = J_{\mathrm{t}}\dot{\omega}_{\mathrm{t}} \tag{6}$$

where P_{Ap} (Pa) and P_{Bp} (Pa) are respectively the inlet and outlet pressures of the hydraulic pump, c_{fp} (Nm/(rad/s)) and J_{t} (kgm^2) are respectively the friction coefficient and inertia of the two coupled components, D_{p} (m^3/rad) is the pump displacement. The pump displacement can be continuously varied by regulating a displacement control mechanism that has significantly faster dynamics than the HTT and is thus modelled as a proportional element as

$$D_{\mathrm{p}} = k_{\mathrm{p}} \cdot u_{\mathrm{p}} \tag{7}$$

where k_{p} (m^3/rad/V) and u_{p} (V) are respectively the constant pump displacement gradient and pump control input.

The hydraulic pump flowrate Q_{p} (m^3/s) is formulated based on continuity equations [24] as

$$Q_{\mathrm{p}} = D_{\mathrm{p}}\omega_{\mathrm{t}} - c_{\mathrm{pL}}\left(P_{\mathrm{Ap}} - P_{\mathrm{Bp}}\right) \tag{8}$$

where c_{pL} (m^3/s/Pa) is the pump's leakage coefficient.

C. The Accumulator

By assuming the pressures $P_{\mathrm{Ap}} \geq P_{\mathrm{Bp}}$, the flowrate Q_{acc} of the high-pressure hydraulic accumulator can be formulated as [25]

$$Q_{\mathrm{acc}} = \begin{cases} 0 & \text{if } P_{\mathrm{Ap}} \leq P_{\mathrm{acc}} \\ \dfrac{\mathrm{d}}{\mathrm{d}\,t}\left[V_{\mathrm{acc}}\left(1 - \dfrac{P_{\mathrm{acc}}}{P_{\mathrm{Ap}}}\right)^{\frac{1}{\kappa}}\right] & \text{if } P_{\mathrm{Ap}} > P_{\mathrm{acc}}. \end{cases} \tag{9}$$

where V_{acc} (m^3) and P_{acc} (Pa) are respectively the preset volume and pressure of the hydraulic accumulator, κ is a adiabatic coefficient.

D. The Hydraulic Motor and Pipelines

The in-out flow rate Q_{m} of the hydraulic motor can be derived as follows

$$Q_{\mathrm{m}} = D_{\mathrm{m}}\omega_{\mathrm{g}} + c_{\mathrm{mL}}\left(P_{\mathrm{Am}} - P_{\mathrm{Bm}}\right) + \frac{V_{\mathrm{o}}}{\beta_{\mathrm{e}}}\left(\dot{P}_{\mathrm{Am}} - \dot{P}_{\mathrm{Bm}}\right) \tag{10}$$

where P_{Am} (Pa) and P_{Bm} (Pa) are respectively the inlet and outlet pressures of the hydraulic motor, c_{mL} (m^3/s/Pa) and ω_{g} (rad/s) are respectively the leakage coefficient and motor/generator rotation speed, V_{o} (m^3) and β_{e} (Pa) are respectively the volume of the hydraulic motor and the effective elastic modulus, D_{m} (m^3/rad) is the hydraulic motor displacement.

The variable displacement control mechanism of the hydraulic motor also has faster dynamics than the HTT, and can thus be simplified as a proportional element as

$$D_{\mathrm{m}} = k_{\mathrm{m}} \cdot u_{\mathrm{m}} \tag{11}$$

where k_{m} (m[3]/rad/V) and u_{m} (V) are respectively the constant motor displacement gradient and hydraulic motor control input.

The input torque exerted on the generator shaft is

$$D_{\mathrm{m}}\left(P_{\mathrm{Am}}-P_{\mathrm{Bm}}\right)=J_{\mathrm{g}}\dot{\omega}_{\mathrm{g}}+c_{\mathrm{fg}}\omega_{\mathrm{g}}+T_{\mathrm{g}} \tag{12}$$

where c_{fg} (Nm/(rad/s)) and J_{g} (kgm[2]) are the friction coefficient and the total inertia of the hydraulic motor driven generator, and T_{g} (Nm) is the generator reaction torque.

The relationship between the hydraulic pump port pressures and motor chamber pressures can be approximated as

$$\begin{cases} P_{\mathrm{Ap}}=P_{\mathrm{Am}}+P_{\mathrm{pipe}} \\ P_{\mathrm{Bp}}=P_{\mathrm{Bm}}-P_{\mathrm{pipe}} \end{cases} \tag{13}$$

where P_{pipe} (Pa) is pressure loss of the pipelines connecting the two hydraulic machines.

Because of the flow continuity of the hydrostatic transmission and negligible pipeline pressure drop $P_{\mathrm{pipe}}=0$, the hydrostatic pressures satisfy the equations $P_{\mathrm{Ap}}\approx P_{\mathrm{Am}}, P_{\mathrm{Bp}}\approx P_{\mathrm{Bm}}$.

E. The Generator and HTT Dynamics

The selected generator holds several advantages including high efficiency and low maintenance cost. Its dynamics are represented by its torque, power equations as follows

$$P_{\mathrm{g}}=T_{\mathrm{g}}\cdot\omega_{\mathrm{g}} \tag{14}$$

where P_{g} (W) and T_{g} (Nm) are respectively the generator power and torque.

In order to obtain the optimal generator torque, by neglecting the friction coefficient in (6), it can be derived that

$$P_{\mathrm{Ap}}-P_{\mathrm{Bp}}=\frac{T_{\mathrm{t}}-J_{\mathrm{t}}s\omega_{\mathrm{t}}}{D_{\mathrm{p}}} \tag{15}$$

where s is the Laplace operator.

Neglecting the pipeline pressure drop and substituting (15) into the Laplace transform of (12) gives

$$T_{\mathrm{g}}\left(s\right)=\frac{D_{\mathrm{m}}}{D_{\mathrm{p}}}\left(T_{\mathrm{t}}-J_{\mathrm{t}}s\omega_{\mathrm{t}}\right)-J_{\mathrm{g}}s\omega_{\mathrm{g}} \tag{16}$$

By considering (4) and (5), one obtains the optimal generator torque

$$T_{\mathrm{gopt}}\left(s\right)=\frac{D_{\mathrm{m}}}{D_{\mathrm{p}}}\left(T_{\mathrm{topt}}-J_{\mathrm{t}}s\omega_{\mathrm{topt}}\right)-J_{\mathrm{g}}s\omega_{\mathrm{gopt}} \tag{17}$$

By equaling the flowrates $Q_{\mathrm{p}}=Q_{\mathrm{m}}$ in (8) and (10) and neglecting the pipeline pressure drop, the generator speed is

$$\begin{cases} \omega_{\mathrm{g}}=\dfrac{D_{\mathrm{p}}}{D_{\mathrm{m}}}\omega_{\mathrm{t}}-\left(\dfrac{c_{\mathrm{pm}}\beta_{\mathrm{e}}+V_{\mathrm{o}}s}{D_{\mathrm{m}}\beta_{\mathrm{e}}}\right)P_{\mathrm{L}} \\ P_{\mathrm{L}}=P_{\mathrm{Am}}-P_{\mathrm{Bm}}=P_{\mathrm{Ap}}-P_{\mathrm{Bp}}. \end{cases} \tag{18}$$

where $c_{\mathrm{pm}}=c_{\mathrm{pL}}+c_{\mathrm{mL}}$.

Therefore, the optimal generator speed can be designed as

$$\omega_{\mathrm{gopt}}=\frac{D_{\mathrm{p}}}{D_{\mathrm{m}}}\omega_{\mathrm{topt}}-\left(\frac{c_{\mathrm{pm}}\beta_{\mathrm{e}}+V_{\mathrm{o}}s}{D_{\mathrm{m}}\beta_{\mathrm{e}}}\right)P_{\mathrm{L}} \tag{19}$$

By considering (14), (17) and (19), the optimal generator power can be expressed as

$$P_{\mathrm{gopt}}=T_{\mathrm{gopt}}\cdot\omega_{\mathrm{gopt}} \tag{20}$$

As shown in (17), (19) and (20), the optimal generator power can be obtained as a function of the optimal turbine rotor speed, the hydraulic pressure and the optimal turbine torque, and can hence be derived accordingly as the reference input for the controller design in the following sections.

IV. Smooth Sliding Mode Observer Design

As shown in Fig. 1, the generator is rigidly coupled to the hydraulic motor and the dynamics of the two components can be described in (12), which can be readily used to estimate the generator torque in real time, thereby eliminating the need to model the generator dynamics in the conventional synchronously rotating d-q reference frame.

Combining (11) and (12) gives

$$\dot{\omega}_{\mathrm{g}}=-\frac{c_{\mathrm{fg}}}{J_{\mathrm{g}}}\omega_{\mathrm{g}}+\frac{k_{\mathrm{m}}P_{\mathrm{L}}}{J_{\mathrm{g}}}u_{\mathrm{m}}-\frac{T_{\mathrm{g}}}{J_{\mathrm{g}}} \tag{21}$$

By re-arranging (21), one obtains

$$\dot{x}_{\mathrm{g}}=f_{\mathrm{g}}\left(x_{\mathrm{g}}\right)+g_{\mathrm{g}}u_{\mathrm{m}}+d_{\mathrm{g}}\left(x_{\mathrm{g}}\right) \tag{22}$$

where

$$\begin{cases} x_{\mathrm{g}}=\omega_{\mathrm{g}};\, f_{\mathrm{g}}\left(x_{\mathrm{g}}\right)=-\dfrac{c_{\mathrm{fg}}}{J_{\mathrm{tg}}}\omega_{\mathrm{g}}; \\ g_{\mathrm{g}}=\dfrac{k_{\mathrm{m}}P_{\mathrm{L}}}{J_{\mathrm{g}}};\, d_{\mathrm{g}}\left(x_{\mathrm{g}}\right)=-\dfrac{T_{\mathrm{g}}}{J_{\mathrm{g}}}. \end{cases} \tag{23}$$

Based on the state space representation in (23), a smooth second order sliding mode observer can be designed as [26]

$$\begin{cases} \dot{z}_0=v_0+f_{\mathrm{g}}\left(x_{\mathrm{g}}\right)+g_{\mathrm{g}}u_{\mathrm{m}} \\ v_0=-\lambda_0L^{\frac{1}{3}}\left|z_0-x_{\mathrm{g}}\right|^{\frac{2}{3}}\operatorname{sign}\left(z_0-x_{\mathrm{g}}\right)+z_1 \\ \dot{z}_1=v_1 \\ v_1=-\lambda_1L^{\frac{1}{2}}\left|z_1-v_0\right|^{\frac{1}{2}}\operatorname{sign}\left(z_1-v_0\right)+z_2 \\ \dot{z}_2=-\lambda_2L\operatorname{sign}\left(z_2-v_1\right) \end{cases} \tag{24}$$

where z_0,v_0,z_0,v_1,z_2 are observer state variables, $\lambda_0,\lambda_1,\lambda_2,L$ are positive design parameters.

Considering the dynamical model governed by (22) and (23), the second-order observer in (24) can estimate the disturbance term $d_{\mathrm{g}}\left(x_{\mathrm{g}}\right)$ in finite time. Thus, when the time $t\to\infty$, the observer states $z_0=x_{\mathrm{g}}, z_1=d_{\mathrm{g}}\left(x_{\mathrm{g}}\right), z_2=\dot{d}_{\mathrm{g}}\left(x_{\mathrm{g}}\right)$. The observer errors will also converge to zero in finite time [27].

Based on the real-time estimated values of the term $d_{\mathrm{g}}\left(x_{\mathrm{g}}\right)$ in (24), the generator torque can be estimated as follows

$$\hat{T}_{\mathrm{g}}=-J_{\mathrm{g}}\cdot\hat{d}_{\mathrm{g}}\left(x_{\mathrm{g}}\right) \tag{25}$$

This shows that the generator torque can be readily estimated from the coupled hydraulic motor-generator dynamics, which avoids explicitly modelling the generator torque in the d-q reference frame.

V. Nonlinear Predictive Control Design

The control objective of the NPC is to find the optimal control inputs for the hydraulic pump and motor when the tidal turbine speed is below rated such that the HTT can operate at the maximum power extraction points. The ADV preview based NPC is a real time optimal control strategy that can fully use the knowledge of future tidal speeds. In contrast to traditional model predictive control that requires resolving a nonlinear dynamic optimization problem online (which requires extensive computation), the proposed NPC can be applied directly to control the fast dynamics of the HTT without online optimizations. The proposed NPC is also able to cope with the nonlinearities and model uncertainties and is sufficiently robust with respect to these uncertainties and disturbances as compared with traditional model predictive control. The proposed NPC design can be divided into the turbine speed control and the generator power control as detailed in the following subsections.

A. The Turbine Speed Control

By combining (6) and (7), the coupled dynamics of the turbine and hydraulic pump are expressed as

$$\dot{\omega}_{\mathrm{t}} = -\frac{c_{\mathrm{fp}}}{J_{\mathrm{t}}}\omega_{\mathrm{t}} - \frac{k_{\mathrm{p}}P_{\mathrm{L}}}{J_{\mathrm{t}}}u_{\mathrm{p}} + \frac{T_{\mathrm{t}}}{J_{\mathrm{t}}} \tag{26}$$

By defining the state variable as the turbine rotation speed, (26) can be expressed in an affine nonlinear form as

$$\dot{x}_{\mathrm{t}} = f_{\mathrm{t}}(x_{\mathrm{t}}) + g_{\mathrm{t}}u_{\mathrm{p}} + d_{\mathrm{t}}(x_{\mathrm{t}}) \tag{27}$$

where x_{t} is the state variable, u_{p} represents the control input for the hydraulic pump and $d_{\mathrm{t}}(x_{\mathrm{t}})$ is the lumped disturbance.

$$\begin{cases} x_{\mathrm{t}} = \omega_{\mathrm{t}};\ f_{\mathrm{t}}(x_{\mathrm{t}}) = -\dfrac{c_{\mathrm{fp}}}{J_{\mathrm{t}}}\omega_{\mathrm{t}}; \\ g_{\mathrm{t}} = -\dfrac{k_{\mathrm{p}}P_{\mathrm{L}}}{J_{\mathrm{t}}};d_{\mathrm{t}}(x_{\mathrm{t}}) = \dfrac{T_{\mathrm{t}}}{J_{\mathrm{t}}}. \end{cases} \tag{28}$$

In order to enhance the robustness of the turbine rotation speed control and guarantee the system stability against disturbance $d_{\mathrm{t}}(x_{\mathrm{t}})$, an integral action of the speed tracking error is incorporated into the control loop. Therefore, the rotation speed tracking errors are defined as

$$\begin{cases} e_{\mathrm{t}} = \omega_{\mathrm{t}} - \omega_{\mathrm{topt}} \\ e_{\mathrm{t0}} = \int_0^t e_{\mathrm{t}}(\tau)\,\mathrm{d}\tau \end{cases} \tag{29}$$

where e_{t} is the turbine speed tracking error and e_{t0} is the integral of the speed tracking error.

By using the ADV preview, the tidal speed of *T* time interval ahead can be readily predicted and thus the tracking errors of *T* time interval ahead can be calculated based on (4). By Taylor expansion, (29) is expanded into second order Taylor series as

$$e_{\mathrm{t0}}(t+T) = e_{\mathrm{t0}}(t) + T\dot{e}_{\mathrm{t0}}(t) + \frac{T^2}{2}\left[f_{\mathrm{t}}(x_{\mathrm{t}}) - \dot{\omega}_{\mathrm{topt}}\right] + \frac{T^2}{2}g_{\mathrm{t}}u_{\mathrm{p}} \tag{30}$$

$$e_{\mathrm{t}}(t+T) = e_{\mathrm{t}}(t) + T\left[f_{\mathrm{t}}(x_{\mathrm{t}}) - \dot{\omega}_{\mathrm{topt}}\right] + Tg_{\mathrm{t}}u_{\mathrm{p}} \tag{31}$$

Based on (27)-(31), the optimal control problem consists in designing a control law u_{popt} that will improve the turbine speed tracking accuracy along the interval [*t*, *t* + *h*], where *h* >0 is a prediction horizon, such that the tracking errors $e_{\mathrm{t}}, e_{\mathrm{t0}}$ can be minimized in advance [28].

As defined in the integral over the time horizon of the speed tracking errors, the cost function to be minimized becomes

$$\begin{aligned} &\min J_{\mathrm{t}}(e_{\mathrm{t}}, e_{\mathrm{t0}}, u_{\mathrm{p}}) \\ &= \frac{1}{2}\int_0^h \begin{pmatrix} e_{\mathrm{t0}}(t+T) \\ e_{\mathrm{t}}(t+T) \end{pmatrix}^{\mathrm{T}} \begin{pmatrix} q_{\mathrm{t1}} & 0 \\ 0 & T^2 q_{\mathrm{t2}} \end{pmatrix} \begin{pmatrix} e_{\mathrm{t0}}(t+T) \\ e_{\mathrm{t}}(t+T) \end{pmatrix} \mathrm{d}T + \frac{1}{2}u_{\mathrm{p}}^{\mathrm{T}} r_{\mathrm{t}} u_{\mathrm{p}} \end{aligned} \tag{32}$$

where $q_{\mathrm{t1}}, q_{\mathrm{t2}}, r_{\mathrm{t}}$ are positive weighting constants that are used to penalize the system state and control actions, respectively.

The above nonlinear optimal control problem can be solved iteratively with the gradient descent approach as follows

$$\frac{\partial J_{\mathrm{t}}(e_{\mathrm{t}}, e_{\mathrm{t0}}, u_{\mathrm{p}})}{\partial u_{\mathrm{p}}} = 0 \tag{33}$$

By solving (33), one obtains

$$u_{\mathrm{popt}} = -g_{\mathrm{t}}^{-1}p_{\mathrm{t}}^{-1}\begin{bmatrix} \dfrac{h^3}{6}q_{\mathrm{t1}}e_{\mathrm{t0}}(t) + \dfrac{h^4}{8}(q_{\mathrm{t1}} + 2q_{\mathrm{t2}})e_{\mathrm{t}}(t) + \\ \dfrac{h^5}{20}(q_{\mathrm{t1}} + 4q_{\mathrm{t2}})\left(f_{\mathrm{t}}(x_{\mathrm{t}}) - \dot{\omega}_{\mathrm{topt}}\right) \end{bmatrix} \tag{34}$$

where

$$p_{\mathrm{t}} = \frac{h^5}{20}(q_{\mathrm{t1}} + 4q_{\mathrm{t2}}) + g_{\mathrm{t}}^{-2}r_{\mathrm{t}} \tag{35}$$

The parameters $q_{\mathrm{t1}}, q_{\mathrm{t2}}, r_{\mathrm{t}}$ are chosen to satisfy the constraints on the variable displacement control mechanism of the hydraulic pump and improve the robustness of the proposed controller with respect to model uncertainties and disturbances.

B. The Generator Power Control

The objective of the ADV preview based predictive control is to track the optimal generator power defined in (20) by regulating the hydraulic motor displacement regardless of model uncertainties and disturbances.

For the proposed control, since the $\ell_{g_{\mathrm{g}}}P_g \neq 0$ (ℓ denotes the Lie derivative), the relative degree of generator power output is 1 and thus the nonlinear dynamics model of the generator power can be reorganized based on (14), (22) and (23) as

$$\begin{cases} \dot{P}_{\mathrm{g}} = \ell_{f_{\mathrm{g}}(x_{\mathrm{g}})}P_{\mathrm{g}} + \ell_{g_{\mathrm{g}}}P_{\mathrm{g}}u_{\mathrm{m}} + \ell_{d_{\mathrm{g}}(x_{\mathrm{g}})}P_{\mathrm{g}} + \dot{T}_{\mathrm{g}}\omega_{\mathrm{g}} \\ \ell_{f_{\mathrm{g}}(x_{\mathrm{g}})}P_{\mathrm{g}} = f_{\mathrm{g}}(x_{\mathrm{g}})T_{\mathrm{g}};\ell_{g_{\mathrm{g}}}P_{\mathrm{g}} = g_{\mathrm{g}}T_{\mathrm{g}};\ell_{d_{\mathrm{g}}(x_{\mathrm{g}})}P_{\mathrm{g}} = d_{\mathrm{g}}(x_{\mathrm{g}})T_{\mathrm{g}}. \end{cases} \tag{36}$$

which with uncertainties can be rewritten as

$$\begin{cases} \dot{x}_{\mathrm{pg}} = f_{\mathrm{pg}}(x_{\mathrm{pg}}) + g_{\mathrm{pg}}u_{\mathrm{m}} + d_{\mathrm{pg}}(x_{\mathrm{pg}}) \\ x_{\mathrm{pg}} = P_{\mathrm{g}},\ f_{\mathrm{pg}}(x_{\mathrm{pg}}) = \ell_{f_{\mathrm{g}}(x_{\mathrm{g}})}P_g; \\ g_{\mathrm{pg}} = \ell_{g_{\mathrm{g}}}P_g;d_{\mathrm{pg}}(x_{\mathrm{pg}}) = \ell_{d_{\mathrm{g}}(x_{\mathrm{g}})}P_g + \dot{T}_{\mathrm{g}}\omega_{\mathrm{g}} \end{cases} \tag{37}$$

where x_{pg}, u_{m}, $d_{\mathrm{pg}}(x_{\mathrm{pg}})$ are respectively the system state, effective hydraulic motor displacement control input, lumped non-affine term including external disturbance, and the measurable output is the generator power.

In order to find appropriate control inputs that improve the optimal generator power tracking accuracy in a fixed time interval *T*, the generator power tracking errors are augmented with integral actions and the tracking errors become

$$\begin{cases} e_{\mathrm{pg}} = P_{\mathrm{g}} - P_{\mathrm{gopt}} \\ e_{\mathrm{pg0}} = \int_0^t e_{\mathrm{pg}}(\tau)\,\mathrm{d}\tau \end{cases} \tag{38}$$

where $e_{\mathrm{pg}}, e_{\mathrm{pg0}}$ are respectively the generator power tracking error and error integral.

By using the knowledge of future upstream tidal speeds based on the ADV preview, the tracking errors in (38) can be expanded in the second order Taylor series such that the tracking errors at the T time interval ahead can then be predicted as a function of tracking errors at time instant t. Thus,

$$e_{\mathrm{pg0}}(t+T)=e_{\mathrm{pg0}}(t)+T\dot{e}_{\mathrm{pg0}}(t)+\frac{T^2}{2}\left[f_{\mathrm{pg}}(x_{\mathrm{pg}})-\dot{P}_{\mathrm{gopt}}\right]+\frac{T^2}{2}g_{\mathrm{pg}}u_{\mathrm{m}} \tag{39}$$

$$e_{\mathrm{pg}}(t+T)=e_{\mathrm{pg}}(t)+T\left[f_{\mathrm{pg}}(x_{\mathrm{pg}})-\dot{P}_{\mathrm{gopt}}\right]+Tg_{\mathrm{pg}}u_{\mathrm{m}} \tag{40}$$

In a receding horizon control fashion, the following quadratic function and optimization problem is reformulated as

$$\begin{aligned}&\min J_{\mathrm{pg}}(e_{\mathrm{pg}},e_{\mathrm{pg0}},u_{\mathrm{m}})\\&=\frac{1}{2}\int_0^h\begin{pmatrix}e_{\mathrm{pg0}}(t+T)\\e_{\mathrm{pg}}(t+T)\end{pmatrix}^{\mathrm{T}}\begin{pmatrix}q_{\mathrm{pg1}}&0\\0&T^2q_{\mathrm{pg2}}\end{pmatrix}\begin{pmatrix}e_{\mathrm{pg0}}(t+T)\\e_{\mathrm{pg}}(t+T)\end{pmatrix}\mathrm{d}T+\frac{1}{2}u_{\mathrm{m}}^{\mathrm{T}}r_{\mathrm{pg}}u_{\mathrm{m}}\end{aligned} \tag{41}$$

where $q_{\mathrm{pg1}}, q_{\mathrm{pg2}}, r_{\mathrm{pg}}$ are constant weighting coefficients.

Following the same gradient descent procedure as in (33), the optimal control for the hydraulic motor displacement that minimizes the cost function (41) can be obtained as

$$\frac{\partial J_{\mathrm{pg}}(e_{\mathrm{pg}},e_{\mathrm{pg0}},u_{\mathrm{m}})}{\partial u_{\mathrm{m}}}=0 \tag{42}$$

By solving (42), the unique optimal control signal u_{mopt} subject to (39)-(41) can be calculated as

$$u_{\mathrm{mopt}}=-\hat{g}_{\mathrm{pg}}^{-1}\hat{p}_{\mathrm{pg}}^{-1}\begin{bmatrix}\frac{h^3}{6}q_{\mathrm{pg1}}e_{\mathrm{pg0}}(t)+\frac{h^4}{8}(q_{\mathrm{pg1}}+2q_{\mathrm{pg2}})e_{\mathrm{pg}}(t)+\\\frac{h^5}{20}(q_{\mathrm{pg1}}+4q_{\mathrm{pg2}})\left(f_{\mathrm{pg}}(x_{\mathrm{pg}})-\dot{P}_{\mathrm{gopt}}\right)\end{bmatrix} \tag{43}$$

where $\hat{g}_{\mathrm{pg}}=g_{\mathrm{pg}}-\tilde{g}_{\mathrm{pg}}$ is the estimated value of g_{pg} by using the estimated generator torque in (25), and $\tilde{g}_{\mathrm{pg}}$ is the estimation error of $\hat{g}_{\mathrm{pg}}$.

$$p_{\mathrm{pg}}=\frac{h^5}{20}(q_{\mathrm{pg1}}+4q_{\mathrm{pg2}})+\hat{g}_{\mathrm{pg}}^{-2}r_{\mathrm{pg}} \tag{44}$$

The parameters $q_{\mathrm{pg1}}, q_{\mathrm{pg2}}, r_{\mathrm{pg}}$ can be tuned to reduce the computational burden of NPC with long prediction horizons and simultaneously satisfy the constraints on the variable displacement control mechanism of the hydraulic motor [29]. Actually, the optimal values in (43) can be repeatedly obtained at every instant t ahead of the current state.

C. Stability Analysis

The stability of the overall closed control system involving the turbine speed control and the generator power control can be proved based on the system tracking error dynamics.

Define $\boldsymbol{e}_1=[\boldsymbol{e}_{\mathrm{t0}}, \boldsymbol{e}_{\mathrm{pg0}}]^{\mathrm{T}}$, $\boldsymbol{e}_2=[e_{\mathrm{t}}, e_{\mathrm{pg}}]^{\mathrm{T}}$, $\boldsymbol{P}=\mathrm{diag}\{p_{\mathrm{t}}, p_{\mathrm{pg}}\}$, $\boldsymbol{Q}_1=\mathrm{diag}\{q_{\mathrm{t1}}, q_{\mathrm{pg1}}\}$, $\boldsymbol{Q}_2=\mathrm{diag}\{q_{\mathrm{t2}}, q_{\mathrm{pg2}}\}$, $\boldsymbol{R}=\mathrm{diag}\{r_{\mathrm{t}}, r_{\mathrm{pg}}\}$ and $\boldsymbol{M}=\mathrm{diag}\{g_{\mathrm{t}}^{-1}, g_{\mathrm{pg}}^{-1}\}$. By substituting (34) and (43) into (27) and (37) respectively, error dynamics in (29) and (38) are re-arranged as

$$\begin{cases}\dot{\boldsymbol{e}}_1=\boldsymbol{e}_2\\\dot{\boldsymbol{e}}_2=-\frac{h^3}{6}\boldsymbol{P}^{-1}\boldsymbol{Q}_1\boldsymbol{e}_1-\frac{h^4}{8}\boldsymbol{P}^{-1}(\boldsymbol{Q}_1+2\boldsymbol{Q}_2)\boldsymbol{e}_2+\boldsymbol{P}^{-1}\boldsymbol{MRM}(\boldsymbol{f}-\dot{\boldsymbol{x}}_{\mathrm{opt}})+\boldsymbol{d}\end{cases} \tag{45}$$

where $\boldsymbol{f}=\left[f_{\mathrm{t}}(x_{\mathrm{t}}), f_{\mathrm{pg}}(x_{\mathrm{pg}})\right]^{\mathrm{T}}$, $\dot{\boldsymbol{x}}_{\mathrm{opt}}=\left[\dot{\omega}_{\mathrm{topt}}, \dot{P}_{\mathrm{gopt}}\right]^{\mathrm{T}}$, $\boldsymbol{d}=\left[d_{\mathrm{t}}(x_{\mathrm{t}}), d_{\mathrm{pg}}(x_{\mathrm{pg}})+\tilde{g}_{\mathrm{pg}}u_{\mathrm{mopt}}\right]^{\mathrm{T}}$.

By defining $\boldsymbol{e}=[\boldsymbol{e}_1, \boldsymbol{e}_2]^{\mathrm{T}}$, the tracking error equation (45) can be written in a compact form as

$$\begin{cases}\dot{\boldsymbol{e}}=\boldsymbol{\Lambda e}+\boldsymbol{\Delta}\\\boldsymbol{\Lambda}=\begin{bmatrix}0&\boldsymbol{I}_2\\-\frac{h^3}{6}\boldsymbol{P}^{-1}\boldsymbol{Q}_1&-\frac{h^4}{8}\boldsymbol{P}^{-1}(\boldsymbol{Q}_1+2\boldsymbol{Q}_2)\end{bmatrix}\\\boldsymbol{\Delta}=\boldsymbol{P}^{-1}\boldsymbol{MRM}(\boldsymbol{f}-\dot{\boldsymbol{x}}_{\mathrm{opt}})+\boldsymbol{d}\end{cases} \tag{46}$$

Define a Lyapunov function candidate for the augmented error dynamics system in (46) as follows

$$V(\boldsymbol{e})=\boldsymbol{e}^{\mathrm{T}}\boldsymbol{P}_{\mathrm{A}}\boldsymbol{e} \tag{47}$$

where $\boldsymbol{P}_{\mathrm{A}}$ is a constant symmetric and positive definite matrix.

The time differentiation of (47) along the error vector dynamics in (46) gives

$$\begin{aligned}\dot{V}(\boldsymbol{e})&=\boldsymbol{e}^{\mathrm{T}}\left(\boldsymbol{\Lambda}^{\mathrm{T}}\boldsymbol{P}_{\mathrm{A}}+\boldsymbol{P}_{\mathrm{A}}\boldsymbol{\Lambda}\right)\boldsymbol{e}+2\boldsymbol{\Delta}^{\mathrm{T}}\boldsymbol{P}_{\mathrm{A}}\boldsymbol{e}\\&=-\boldsymbol{e}^{\mathrm{T}}\boldsymbol{Q}_{\mathrm{A}}\boldsymbol{e}+2\boldsymbol{\Delta}^{\mathrm{T}}\boldsymbol{P}_{\mathrm{A}}\boldsymbol{e}\le-\lambda_{\min}(\boldsymbol{Q}_{\mathrm{A}})\|\boldsymbol{e}\|^2+2\lambda_{\max}(\boldsymbol{P}_{\mathrm{A}})\|\boldsymbol{\Delta}\|\|\boldsymbol{e}\|\end{aligned} \tag{48}$$

where $\boldsymbol{Q}_{\mathrm{A}}=-\boldsymbol{\Lambda}^{\mathrm{T}}\boldsymbol{P}_{\mathrm{A}}-\boldsymbol{P}_{\mathrm{A}}\boldsymbol{\Lambda}$ is a symmetric positive-definite matrix.

By using Young's inequality, one obtains

$$2\lambda_{\max}(\boldsymbol{P}_{\mathrm{A}})\|\boldsymbol{\Delta}\|\|\boldsymbol{e}\|\le\sigma\lambda_{\min}(\boldsymbol{Q}_{\mathrm{A}})\|\boldsymbol{e}\|^2+\frac{\lambda_{\max}^2(\boldsymbol{P}_{\mathrm{A}})\|\boldsymbol{\Delta}\|^2}{\sigma\lambda_{\min}(\boldsymbol{Q}_{\mathrm{A}})} \tag{49}$$

where $0<\sigma<1$ is a constant, $\lambda_{\max}(\bullet), \lambda_{\min}(\bullet)$ are respectively the largest and smallest eigenvalues of the matrix $(\bullet)$, $\|\bullet\|$ is the Euclidean norm of the matrix $(\bullet)$.

Based on (49), reformulate the time derivative in (48) as

$$\begin{aligned}\dot{V}(\boldsymbol{e})&\le-(1-\sigma)\lambda_{\min}(\boldsymbol{Q}_{\mathrm{A}})\|\boldsymbol{e}\|^2+\frac{\lambda_{\max}^2(\boldsymbol{P}_{\mathrm{A}})\|\boldsymbol{\Delta}\|^2}{\sigma\lambda_{\min}(\boldsymbol{Q}_{\mathrm{A}})}\\&\le-\frac{(1-\sigma)\lambda_{\min}(\boldsymbol{Q}_{\mathrm{A}})}{\lambda_{\max}(\boldsymbol{P}_{\mathrm{A}})}\boldsymbol{V}(\boldsymbol{e})+\frac{\lambda_{\max}^2(\boldsymbol{P}_{\mathrm{A}})\|\boldsymbol{\Delta}\|^2}{\sigma\lambda_{\min}(\boldsymbol{Q}_{\mathrm{A}})}\\&=-aV(\boldsymbol{e})+b\end{aligned} \tag{50}$$

The solution of (50) is

$$V(t)\le V(0)\exp(-at)+\frac{b}{a}[1-\exp(-at)] \tag{51}$$

where a and b are positive constants defined as

$$a=\frac{(1-\sigma)\lambda_{\min}(\boldsymbol{Q}_{\mathrm{A}})}{\lambda_{\max}(\boldsymbol{P}_{\mathrm{A}})};b=\frac{\lambda_{\max}^2(\boldsymbol{P}_{\mathrm{A}})\|\boldsymbol{\Delta}\|^2}{\sigma\lambda_{\min}(\boldsymbol{Q}_{\mathrm{A}})}. \tag{52}$$

As time $t\rightarrow\infty$, based on (51) and (52), the tracking error vector $\boldsymbol{e}$ is uniformly ultimately bounded as

$$\|\boldsymbol{e}\|\le\frac{\lambda_{\max}(\boldsymbol{P}_{\mathrm{A}})}{\lambda_{\min}(\boldsymbol{Q}_{\mathrm{A}})}\frac{\|\boldsymbol{\Delta}\|}{\sqrt{\sigma(1-\sigma)}}\sqrt{\frac{\lambda_{\max}(\boldsymbol{P}_{\mathrm{A}})}{\lambda_{\min}(\boldsymbol{P}_{\mathrm{A}})}} \tag{53}$$

As shown in (53), the bound of the tracking error vector depends on the magnitude of the parameters a and b. Consequently, by properly selecting the parameters a and b, $V_e(t)$ will be bounded by b/a when $t\rightarrow\infty$ and the tracking errors in (53) will be significantly reduced and will hence converge to zero in finite time regardless of model uncertainties and external disturbances. By LaSalle's invariance theorem [30], the tracking errors tend to the invariant and the origin of (46) $\boldsymbol{e}=0$ is globally asymptotically stable.

VI. Case Study and Validations

A 150 kW HTT was designed and modelled in Simulink/ Simscape as a case study to investigate the HTT dynamics and the performances of the ADV preview based NPC in maximizing tidal power generations, which will be compared with the case with non-predictive control.

A. Design Experiments

The 150 kW HTT was designed as a horizontal tidal turbine integrated with hydrostatic transmission as illustrated in Fig. 1. The main components of the HTT were constructed by using the Simulink Simscape Fluids, hydraulics and power system library. The tests were conducted under the rated tidal speed of 2 m/s to quantify the effects of the proposed predictive control in maximizing tidal power generations. The tidal turbine blade radius is designed as 5 m and thus the HTT power generation under the rated tidal speed is 150 kW as evidenced in section III. The optimal tip speed ratio is designed as 8 for the optimal turbine rotor power generation. The rated generator torque is 800 Nm, and the rated hydrostatic pressure difference $P_{\mathrm{Ap}} - P_{\mathrm{Bp}} = P_{\mathrm{Am}} - P_{\mathrm{Bm}} = P_{\mathrm{L}} = 5\times10^{7}$ Pa.

The proposed HTT was tested with and without preview information of the tidal speed. The main parameters of the ADV preview based predictive control in (34) and (43) are set as $q_{\mathrm{t1}}=1.55, q_{\mathrm{t2}}=5.5, r_{\mathrm{t}}=0.02$ and $q_{\mathrm{pg1}}=3.4, q_{\mathrm{pg2}}=1.98, r_{\mathrm{pg}}=0.02$, and the prediction horizon h is set as 5 sampling intervals while the sampling interval is 0.001 s in all the tests. The values of $q_{\mathrm{t1}}, q_{\mathrm{t2}}, r_{\mathrm{t}}$ and $q_{\mathrm{pg1}}, q_{\mathrm{pg2}}, r_{\mathrm{pg}}$ can be gradually increased from zero until the closed loop HTT system can track the optimal turbine rotation speed and the optimal generator power without obvious oscillations. The maximum values of these parameters should also be chosen such that actuation control signals of the hydraulic pump and motor displacements are not saturated.

The generator torque estimations based on the smooth second order sliding mode observer designed in section IV were included in the NPC problem in a straightforward and systematic way. The parameters of the sliding mode observer were set to relatively large values to increase the estimation accuracy and reduce the computational burden of NPC. The observer parameters are set to be $\lambda_0=600, \lambda_1=862, \lambda_2=1000, L=2$.

The non-predictive control used for comparison is a simple proportional–integral controller that has been designed to maintain the optimal tip speed ratio and the optimal generator power tracking based on real-time measurements from the turbine. The controller is configured as follows.

$$\begin{cases} u_{\mathrm{p}} = K_{\mathrm{pt}} e_{\mathrm{t}} + K_{\mathrm{it}} e_{\mathrm{t0}} \\ u_{\mathrm{m}} = K_{\mathrm{pg}} e_{\mathrm{pg}} + K_{\mathrm{ig}} e_{\mathrm{pg0}} \end{cases} \tag{54}$$

where $K_{\mathrm{pt}}, K_{\mathrm{it}}$ and $K_{\mathrm{pg}}, K_{\mathrm{ig}}$ are respectively proportional and integral gains for the turbine rotation speed and generator power control. The control gains are tuned by using the Ziegler-Nichols tuning method [31] while satisfying the actuation control constraints on the hydraulic pump and motor displacements.

B. Results and Discussions

As shown in Fig. 2, a 120 s tidal stream speed is directly collected from real ocean conditions from the East China Sea by using ADV, and is considered to vary under the rated value of 2 m/s as input for the HTT. The ADV was located a short horizontal distance ahead of the turbine hub height point to provide tidal preview information as input for designing and implementing the proposed NPC. The ADV measured tidal stream speed data have the longitudinal turbulence intensity of around 5% and normally have a small error distribution since the ADV cannot be calibrated to the ideal condition.

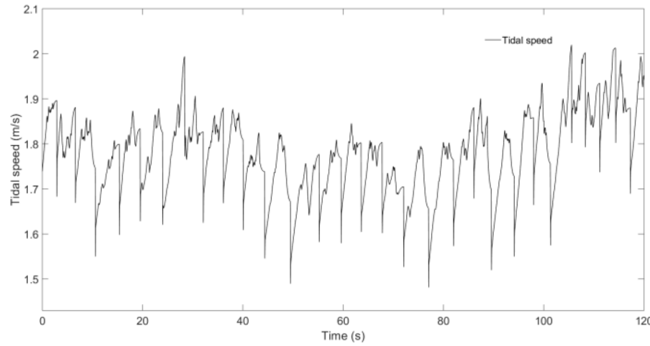

Fig. 2 The tidal speed variations

As shown in Fig. 3, the turbine rotor speed of the HTT can much more accurately track the optimal speed when using the ADV preview based NPC than the case with non-predictive control. This result is attributed to the fact that the preview based NPC can fully make use of the measurements of the approaching tidal speed field in advance to improve the control efficiency and accuracy in comparison with the non-predictive control, which demonstrates the theoretical results in section V.

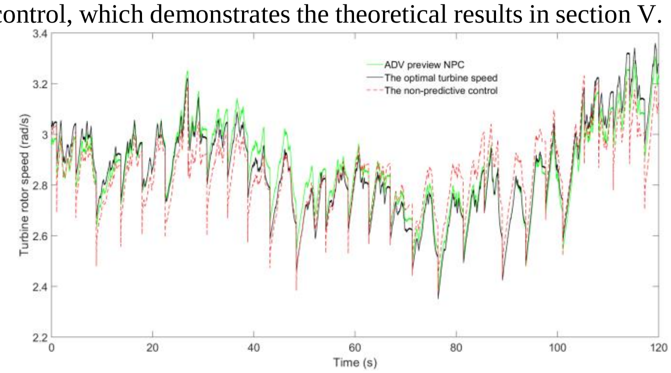

Fig. 3 The turbine rotor speed variations

The effects of ADV preview control are also quantified with respect to the generator power. As shown in Fig. 4, the optimal generator power calculated in (20) can be more accurately tracked by using the preview NPC than the case without predictive control. The maximum generator power around the rated tidal speed is around 130 kW, which implies that the HTT has a relatively high power transmission efficiency of around 87% around the rated tidal speed of 2 m/s.

The averaged generator power in the simulation horizon is

$$\bar{P}_{\mathrm{g}} = \frac{1}{N}\sum_{i=1}^{N} P_{\mathrm{g}i} \tag{55}$$

where N is the number of sample data points and $P_{\mathrm{g}i}$ is the generator power at the sample data point i. $\bar{P}_{\mathrm{g}}$ is used to further evaluate the efficiency of the controller.

The calculated results based on (55) reveal that the averaged generator power can be increased by 6.76% with the preview control in comparison with the non-predictive control. The results also suggest that the power generation efficiency of the HTT can be increased by 6.76% by using the preview control as compared with the non-predictive control since the comparisons are made under the same tidal stream condition. As a result, the HTT controlled by the classical non-predictive control method can achieve the power generation efficiency of around 80% at the rated tidal speed of 2 m/s.

The above comparison results reveal the ADV preview NPC can fully use the knowledge of future tidal speeds and can response in advance to track the optimal generator power points than the non-predictive control, and hence the control accuracy and efficiency will be highly improved. The results are also highly consistent with that in Fig. 3 and the theoretical results in section V, and hence suggest that ADV preview can help to increase the HTT power generation while mitigating generator power fluctuations during large tidal speed variations.

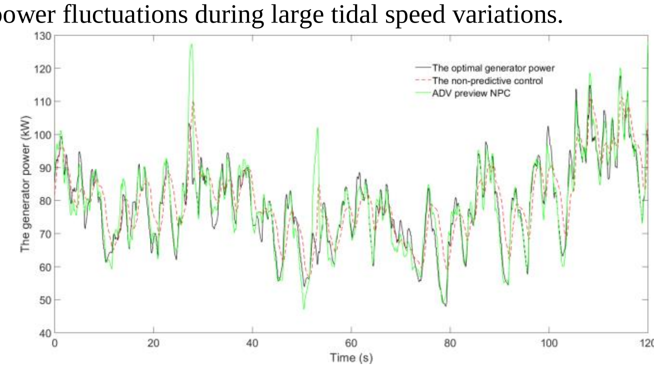

Fig. 4 The generator power variations

The performance of the smooth second order sliding mode observer was also evaluated, assuming large turbine disturbances including un-modelled dynamics and frictions, etc. The estimation error rate (ERR) is used to measure the estimation performances of the observer:

$$\text{ERR} = \frac{\bullet_i - \hat{\bullet}_i}{\bullet_i} \times 100\% \tag{56}$$

where $\bullet$ is the real values representing T_{g} or ω_{g}, $\hat{\bullet}$ is observer estimates representing $\hat{T}_{\text{g}}$ or $\hat{\omega}_{\text{g}}$, and i is the index of the sample points in the simulation horizon.

As shown in Fig. 5, the generator torque varies between 200 Nm and 800 Nm and the estimated generator torque always tracks the real values with high accuracy which can be more than 90%. The torque estimation error rates as shown in Fig. 8 can also be well maintained within ±10% despite the two spikes around 30 s and 50 s due to the sudden changes of the generator torque. Therefore, the effectiveness of the designed sliding mode observer is readily validated and the estimated torque is highly accurate to be used in the NPC design in section V-B.

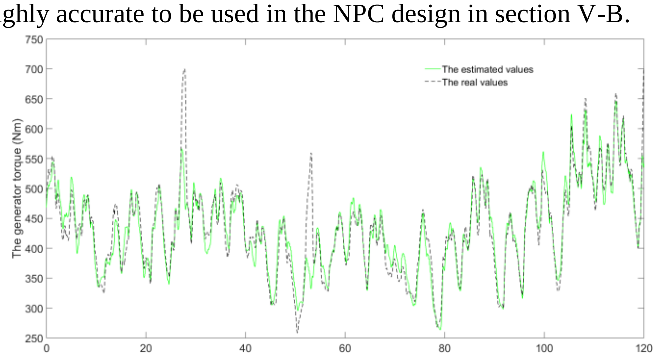

Fig. 5 The generator torque variations

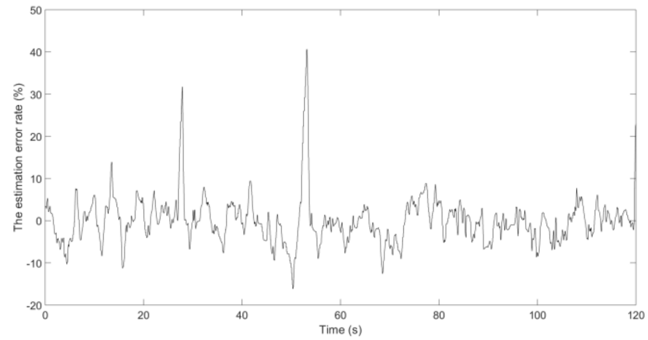

Fig. 6 The generator torque estimation error rates

The generator speed is also estimated by using the smooth second order sliding mode observer designed in section IV and the state z_0 is used to estimate the generate speed which is x_{g} in (22). As illustrated in Fig. 7, the generator speed estimates on the basis of sliding mode observer are very close to the real values. The speed estimation error rates as shown in Fig. 8 can almost be kept within ±0.6%, which is very close to 0 and hence indicates that the designed observer is accurate enough in estimating the fast generator dynamics. The highly accurate estimates increase the control performance for the NPC loop to cope with the non-linear nature of the HTT dynamics, model uncertainties and various disturbances in advance by incorporating previewed tidal speed measurements.

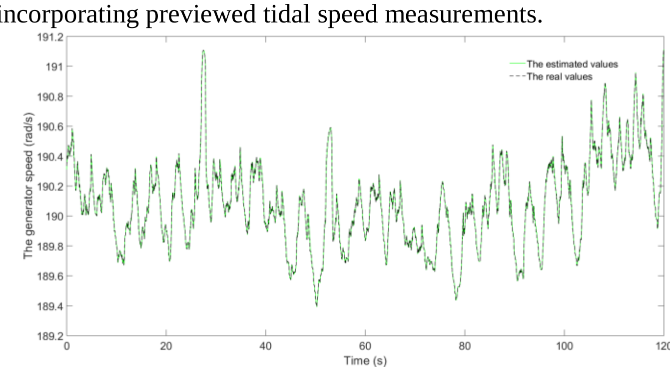

Fig. 7 The generator speed variations

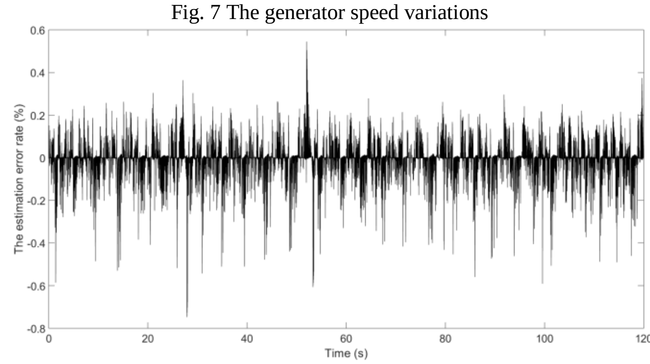

Fig. 8 The generator speed estimation error rates

VII. Conclusion

This paper has shown the benefits of using the NPC for the maximum power capture of a HTT when the tidal speed is below rated. The HTT has been designed and its detailed dynamics has been modelled. A smooth second order sliding mode observer has also been designed to estimate the HTT parameters without dynamics modelling. The NPC has been obtained by continuously resolving an optimization problem offline over a fixed time horizon, and the robustness and stability are also rigorously proved and guaranteed. The derived NPC has been applied to a 150 kW HTT to illustrate the effectiveness of the proposed controller in extracting the maximum tidal powers. The test results from realistic tidal conditions have shown that the maximum power points can be better tracked by using the proposed NPC in the face of system uncertainties, external disturbances in comparison with the case without predictive control. Therefore, by incorporating future tidal speed measurements, the proposed NPC is able to anticipate upon future events and thereby significantly improve tidal power generations. The proposed HTT and NPC are effective in handling the issues encountered in current tidal energy developments and therefore have high potential to help tidal energy make more contributions towards the renewable energy targets in the future.

The future work will focus on the experimental validations of the HTT and the preview NPC. Another future direction is to include an experimental control program with the consideration of reducing fatigue effects and fluid cavitation.

References

[1] Nicholls-Lee R F, Turnock S R, Boyd S W. Application of bend-twist coupled blades for horizontal axis tidal turbines. Renewable Energy, 2013, 50: 541-550.

[2] Rourke F O, Boyle F, Reynolds A. Tidal energy update 2009. Applied Energy, 2010, 87(2): 398-409.

[3] https://marineenergy.biz/2015/05/01/video-seagen-s-1-2-mw-tidal-turbine/

[4] http://www.reuk.co.uk/wordpress/tidal/tidel-tidal-turbines/

[5] http://www.emec.org.uk/about-us/our-tidal-clients/open-hydro/

[6] https://marineenergy.biz/2015/02/09/video-deltastream-tidal-technology/

[7] Güney M S, Kaygusuz K. Hydrokinetic energy conversion systems: A technology status review. Renewable and Sustainable Energy Reviews, 2010, 14(9): 2996-3004.

[8] Payne G S, Kiprakis A E, Ehsan M, et al. Efficiency and dynamic performance of Digital Displacement™ hydraulic transmission in tidal current energy converters. Proceedings of the Institution of Mechanical Engineers, Part A: Journal of Power and Energy, 2007, 221(2): 207-218.

[9] Liu H, Li W, Lin Y, et al. Tidal current turbine based on hydraulic transmission system. Journal of Zhejiang University-SCIENCE A, 2011, 12(7): 511-518.

[10] Souf-Aljen A S, Maimun A, Samad R, et al. Dynamic Performance Simulation of Hydraulic Transmission for Low Speed Vertical Axis Marine Current Turbine Using MATLAB Simulink. Jurnal Teknologi, 2015, 74(5).

[11] Whitby B, Ugalde-Loo C E. Performance of pitch and stall regulated tidal stream turbines. IEEE Transactions on Sustainable Energy, 2014, 5(1): 64-72.

[12] Zhou Z, Scuiller F, Charpentier J F, et al. Power limitation control for a PMSG-based marine current turbine at high tidal speed and strong sea state. Electric Machines & Drives Conference (IEMDC), 2013 IEEE International. IEEE, 2013: 75-80.

[13] Motley M R, Barber R B. Passive control of marine hydrokinetic turbine blades. Composite Structures, 2014, 110: 133-139.

[14] Benelghali S, Benbouzid M E H, Charpentier J F, et al. Experimental validation of a marine current turbine simulator: Application to a PMSG-based system second-order sliding mode control. IEEE Trans. Industrial Electronics, 2011, 58(1): 118-126.

[15] Winter A. Speed regulated operation for tidal turbines with fixed pitch rotors. OCEANS 2011. IEEE, 2011: 1-8.

[16] Fall O, Charpentier J F, Nguyen N K, et al. Maximum torque per ampere control strategy of a 5-phase PM generator in healthy and faulty modes for tidal marine turbine application. Power Electronics and Application Conference and Exposition (PEAC), 2014 International. IEEE, 2014: 468-473.

[17] Schlipf D, Schlipf D J, Kühn M. Nonlinear model predictive control of wind turbines using LIDAR. Wind Energy, 2013, 16(7): 1107-1129.

[18] Wang N, Johnson K E, Wright A D. FX-RLS-based feedforward control for LIDAR-enabled wind turbine load mitigation. IEEE Transactions on Control Systems Technology, 2012, 20(5): 1212-1222.

[19] Laks J, Pao L, Wright A, et al. The use of preview wind measurements for blade pitch control. Mechatronics, 2011, 21(4): 668-681.

[20] Kristalny M, Madjidian D, Knudsen T. On using wind speed preview to reduce wind turbine tower oscillations. IEEE Transactions on Control Systems Technology, 2013, 21(4): 1191-1198.

[21] Xiao S, Geng H, Yang G. Non-linear pitch control of wind turbines for tower load reduction. IET Renewable Power Generation, 2014, 8(7): 786-794.

[22] Voulgaris G, Trowbridge JH. Evaluation of the acoustic Doppler velocimeter (ADV) for turbulence measurements. Journal of Atmospheric and Oceanic Technology, 1998, 15, 272-89.

[23] Ghefiri K, Bouallègue S, Haggège J. Modeling and SIL simulation of a Tidal Stream device for marine energy conversion. Renewable Energy Congress (IREC), 2015 6th International. IEEE, 2015: 1-6.

[24] Mohammadnejad T, Andrade J E. Numerical modeling of hydraulic fracture propagation, closure and reopening using XFEM with application to in-situ stress estimation. International Journal for Numerical and Analytical Methods in Geomechanics, 2016, 40(15): 2033-2060.

[25] H. E. Merritt, Hydraulic Control Systems. New York, NY, USA: Wiley, 1967.

[26] Hu Q, Li B, Qi J. Disturbance observer based finite-time attitude control for rigid spacecraft under input saturation. Aerospace Science and Technology, 2014, 39: 13-21.

[27] Shtessel Y B, Shkolnikov I A, Levant A. Smooth second-order sliding modes: Missile guidance application. Automatica, 2007, 43(8): 1470-1476.

[28] Hedjar R, Boucher P. Nonlinear receding-horizon control of rigid link robot manipulators. International journal of advanced robotic systems, 2005, 2(1): 3.

[29] Lu P. Non-linear systems with control and state constraints. Optimal Control Applications and Methods, 1997, 18(5): 313-326.

[30] Mancilla-Aguilar J L, García R A. An extension of LaSalle's invariance principle for switched systems. Systems & Control Letters, 2006, 55(5): 376-384.

[31] Hägglund T, Åström K J. Revisiting the Ziegler - Nichols tuning rules for PI control. Asian Journal of Control, 2002, 4(4): 364-380.

Xiuxing Yin received his Ph. D. in mechatronic engineering from Zhejiang University, Hangzhou, China in 2016. He is now a research fellow at the University of Warwick, U. K. His research interests focus on mechatronics, renewable energy and nonlinear control.

Xiaowei Zhao is Professor of Control Engineering at the School of Engineering, University of Warwick. He obtained his PhD degree in Control Theory from Imperial College London. After that he worked as a postdoctoral researcher at the University of Oxford for three years before joining Warwick in 2013. His research interests include (1) control of wind/tidal turbines/farms; (2) grid integration of renewable energy; (3) microgrid; (4) control of fluid-structure interaction with applications to large and flexible wind turbines, highly flexible aircraft, and long-span suspension bridges; (5) control of coupled infinite-dimensional systems.